Molecular Biology of the Cell
Vol. 20, 134–145, January 1, 2009

The Anaphase Promoting Complex Targeting Subunit Ama1 Links Meiotic Exit to Cytokinesis during Sporulation in *Saccharomyces cerevisiae*

Aviva E. Diamond,* Jae-Sook Park,* Ichiro Inoue,† Hiroyuki Tachikawa,† and Aaron M. Neiman*

*Department of Biochemistry and Cell Biology, Stony Brook University, Stony Brook, NY 11794-5215; and †Laboratory of Biological Chemistry, Graduate School of Agricultural and Life Science, The University of Tokyo, Tokyo 113-8657, Japan

Submitted June 18, 2008; Revised October 6, 2008; Accepted October 9, 2008
Monitoring Editor: Mark J. Solomon

Ascospore formation in yeast is accomplished through a cell division in which daughter nuclei are engulfed by newly formed plasma membranes, termed prospore membranes. Closure of the prospore membrane must be coordinated with the end of meiosis II to ensure proper cell division. *AMA1* encodes a meiosis-specific activator of the anaphase promoting complex (APC). The activity of APC^{Ama1} is inhibited before meiosis II, but the substrates specifically targeted for degradation by Ama1 at the end of meiosis are unknown. We show here that *ama1*Δ mutants are defective in prospore membrane closure. Ssp1, a protein found at the leading edge of the prospore membrane, is stabilized in *ama1*Δ mutants. Inactivation of a conditional form of Ssp1 can partially rescue the sporulation defect of the *ama1*Δ mutant, indicating that an essential function of Ama1 is to lead to the removal of Ssp1. Depletion of Cdc15 causes a defect in meiotic exit. We find that prospore membrane closure is also defective in Cdc15 and that this defect can be overcome by expression of a form of Ama1 in which multiple consensus cyclin-dependent kinase phosphorylation sites have been mutated. These results demonstrate that APC^{Ama1} functions to coordinate the exit from meiosis II with cytokinesis.

INTRODUCTION

On starvation for nitrogen in the presence of a nonfermentable carbon source, diploid cells of the yeast *Saccharomyces cerevisiae* exit vegetative growth and enter a program of meiosis and sporulation to generate haploid spores (Esposito and Klapholz, 1981; Neiman, 2005). The process of spore formation is driven by a cell division in which the daughter cells are formed in the cytoplasm of the mother cell. As cells enter meiosis II, the cytoplasmic faces of the spindle pole bodies are modified so that they become centers of membrane nucleation (Moens, 1971; Moens and Rapport, 1971). Four membranes, termed prospore membranes, are formed, one at each spindle pole (Moens, 1971; Neiman, 1998). As haploid chromosome sets separate within the nucleus in meiosis II, each of the prospore membranes grows to engulf the region of the nucleus adjacent to it. Closure of a prospore membrane around a nascent haploid nucleus completes cell division and is equivalent to cytokinesis in mitotic growth. Once the prospore membrane has closed, the prospore then matures by the deposition of spore wall material into the luminal space between the two membranes derived from the prospore membrane (Lynn and Magee, 1970).

As the prospore membrane expands, its growth is guided in part by proteins found at the lip of the growing membrane, termed the leading edge protein coat (Moreno-Borchart *et al*., 2001). Three components of this coat are known: Don1, Ady3, and Ssp1 (Knop and Strasser, 2000; Moreno-Borchart *et al*., 2001; Nickas and Neiman, 2002). The function of Don1 is unknown, although it may be the most peripheral member of the complex, because it requires both Ady3 and Ssp1 for localization to the leading edge (Moreno-Borchart *et al*., 2001; Nickas and Neiman, 2002). Ady3 may function primarily in promoting mitochondrial segregation into the spore (Suda *et al*., 2007). The critical constituent of the leading edge complex is Ssp1. This protein is required for localization of both Ady3 and Don1 to the leading edge (Moreno-Borchart *et al*., 2001). Moreover, in the absence of *SSP1* prospore membrane growth is abnormal and spore formation is blocked (Nag *et al*., 1997; Moreno-Borchart *et al*., 2001).

Ectopic overexpression of *SSP1* in vegetative cells has been shown to block cell growth by interfering with the fusion of secretory vesicles to the plasma membrane (Maier *et al*., 2007). During sporulation Ssp1 is degraded around the time of prospore membrane closure and mutations that stabilize the protein inhibit sporulation (Maier *et al*., 2007). These results have led to the proposal that removal of Ssp1 from the leading edge regulates the timing of cytokinesis during sporulation (Maier *et al*., 2007).

The anaphase promoting complex (APC) is a multisubunit E3 ubiquitin ligase essential for progression through mitosis (Morgan, 1999). The activity of this complex is regulated by accessory subunits of the Cdc20/Fizzy family that direct it to specific substrates (Morgan, 1999). In vegetatively growing *S. cerevisiae*, Cdc20 and Cdh1 regulate APC activity (Visintin *et al*., 1997). Although both Cdc20 and Cdh1 direct the

This article was published online ahead of print in *MBC in Press* (http://www.molbiolcell.org/cgi/doi/10.1091/mbc.E08–06–0615) on October 22, 2008.

Address correspondence to: Aaron M. Neiman (aaron.neiman@sunysb.edu).

degradation of multiple, overlapping targets, each controls the degradation of a specific target essential for cell division: mitotic cyclins for Cdh1 and securin for Cdc20 (Thornton and Toczyski, 2003). During meiosis, Cdc20 is again important for controlling APC activity (Katis *et al*., 2004; Oelschlaegel *et al*., 2005). No meiotic role for Cdh1 has been described; however, a third family member, *AMA1*, is expressed specifically in meiotic cells (Chu *et al*., 1998; Cooper *et al*., 2000).

Deletion of *AMA1* does not block meiosis, but rather the formation of spores; prospore membranes are formed, but the subsequent formation of spore walls is blocked (Coluccio *et al*., 2004). This result suggests that the critical target(s) of APC^{Ama1} is a protein(s) whose degradation is required to allow spore wall assembly. The identity of these putative targets is unknown.

Ama1 is subject to regulation at several levels. Both transcriptional control and meiosis-specific splicing ensure that the protein is expressed only during sporulation (Chu *et al*., 1998; Cooper *et al*., 2000). Although Ama1 can associate with the APC and direct the degradation of securin both in vivo and in vitro, in a wild-type meiosis APC^{Cdc20} is primarily responsible for securin degradation (Oelschlaegel *et al*., 2005). The activity of APC^{Ama1} is held in check by the Mnd2 subunit of the APC and by the activity of the Clb-Cdc28 kinase (Oelschlaegel *et al*., 2005; Penkner *et al*., 2005). Failure to restrict APC^{Ama1} leads to premature loss of cohesin and chromosome missegregation (Oelschlaegel *et al*., 2005; Penkner *et al*., 2005). Although APC^{Ama1} may contribute to the turnover of Pds1 and cyclins during meiosis, the actions of Mnd2 and Clb-Cdc28 ensure that APC^{Ama1} remains inactive until late meiosis II when Mnd2 dissociates from the APC and Clb-kinase activity decreases, consistent with the primary function of APC^{Ama1} in postmeiotic cells (Dahmann and Futcher, 1995; Rabitsch *et al*., 2001; Coluccio *et al*., 2004; Oelschlaegel *et al*., 2005; Carlile and Amon, 2008).

Meiosis also differs from mitosis in the circuitry that regulates exit from the division. In mitotic cells, exit requires the activity of the Cdc14 protein (Wood and Hartwell, 1982; Taylor *et al*., 1997). Two separate pathways, termed FEAR and MEN, collaborate to regulate Cdc14 (Dumitrescu and Saunders, 2002). *CDC14* is also necessary in meiosis, but regulation of Cdc14 in meiosis is largely or wholly mediated by the FEAR network (Marston *et al*., 2003; Kamieniecki *et al*., 2005). The MEN component *CDC15* is required for sporulation, but this seems to be independent of *CDC14* (Pablo-Hernando *et al*., 2007). In meiotic cells depleted of Cdc15, chromosome segregation proceeds normally as judged by 4,6-diamidino-2-phenylindole (DAPI) staining, but prospore membrane growth is abnormal. Also, spindle disassembly at the end of meiosis II is abnormal, and microtubules accumulate rather than disappear (Pablo-Hernando *et al*., 2007). This last result suggests that a late step in exit from meiosis is defective in this mutant.

The terminal phenotype of *ama1*Δ mutants led to the suggestion that *AMA1* may be required to trigger spore wall assembly after the completion of meiosis (Coluccio *et al*., 2004). We report here that *ama1*Δ mutants are defective at a slightly earlier stage of spore formation, the closure of the prospore membrane. This defect in cytokinesis may account for the spore wall assembly defect in the mutant. The *ama1*Δ mutant stabilizes the leading edge protein complex so that the Ssp1 protein persists in postmeiotic cells and the ring structure of the complex remains intact. The stabilization of Ssp1 is likely directly responsible for the *ama1*Δ cytokinesis defect, because inactivation of a conditional allele of *SSP1* can partially rescue the *ama1*Δ sporulation defect. A *cdc15* mutant defective in exit from meiosis II also displays defects in prospore membrane closure. This closure defect can be suppressed by expression of a mutant form of Ama1 in which all the Cdc28 consensus phosphorylation sites have been mutated. These observations suggest that the primary function of APC^{Ama1} is to coordinate exit from meiosis II with cytokinesis during spore formation.

MATERIALS AND METHODS

Strains and Growth Medium

Unless otherwise noted, standard media and genetic techniques were used (Rose and Fink, 1990). The strains used in this study are listed in Table 1. All strains are in the SK-1 background except for AN390 and the JSP strains, which are hybrids between SK-1 and the S288c background. ADY12 and ADY13 were constructed by polymerase chain reaction (PCR)-mediated knockout of *AMA1* in AN117-4B and AN117-16D, respectively, by using pFa6A CgTRP1 as a template for PCR and oligonucleotides (oligos) F1AMA1 and R1AMA1 in AN117-4B and AN117-16D. ADY64 and ADY65 were constructed in the same manner except pFa6A MX6HIS3 (Longtine *et al*., 1998) was the PCR template. To create TC37 and TC38, oligos HT362 and HT87 were used to amplify the hemagglutinin (HA)-tagging cassette in pFA6a-3xHA-HisMX6 (Longtine *et al*., 1998), and the product was used to transform strain ANT117-4B and AN117-16D, respectively. All PCR-mediated integrations were confirmed by genomic PCR with appropriate primers. ADY183 and ADY184 were obtained as segregants from a cross of TC38 and ADY64. ADY183-AMA1 and ADY184-AMA1 are ADY183 and ADY184 transformed with EcoRV-digested pRS306AMA1. To construct strains ADY216, ADY217, ADY218, and ADY220 the degron cassette in plasmid pKL187PSSP1 was amplified using primers SSP1DegronF and SSP1DegronR and transformed into ADY12, ADY13, AN117-4B, and AN117-16D, respectively. The plasmid pKL142 (Sanchez-Diaz *et al*., 2004), carrying *GAL* promoter driven *UBR1*, was linearized by digestion with PmeI and integrated into strains ADY216, ADY217, ADY218, ADY220, AN117-4B, and AN117-16D to generate ADY221, ADY222, ADY223, ADY224, ADY229, and ADY231, respectively. To create ADY225, ADY226, ADY227, ADY228, ADY230, and ADY232, the plasmid p926 was linearized with NdeI and used to transform ADY221, ADY222, ADY223, ADY224, ADY229, and ADY231, respectively. ADY239 and ADY240 were created by transforming ADY12 and ADY13, with p926 followed by pKL142.

For the FLIP studies, ADY64 was crossed with a strain containing a green fluorescent protein (GFP)-tagged *TEF2* allele from the GFP-tagged collection (Huh *et al*., 2003), and mating of *ama1*Δ::*HIS3 TEF2*::GFP::*his5*$^+$ segregants from this cross produced JSP22. To generate the *CLB2pr-CDC15* strains, the GFP collection strain carrying TEF2::GFP was crossed with AN117-4B, and a segregant from this cross, JSP62, was crossed to a *CLB2pr-CDC15* haploid (Pablo-Hernando *et al*., 2007). JSP64 and JSP65 are segregants from this latter cross. Transformation of JSP64 and JSP65 with PstI linearized YIplac128-AMA1pr-AMA1 or YIplac128-AMA1pr-AMA1-m8 (Oelschlaegel *et al*., 2005) was used to generate the haploid parents for JSP99 and JSP104.

Plasmids

Plasmids used in this study are listed in Table 2. To construct pRS426-R20, the coding region of monomeric red fluorescent protein (mRFP) in a template pTi mRFP (Gao *et al*., 2005) was amplified using primers HNO941 and HNO942, the product was digested with XbaI and EcoRI and used to replace the GFP sequence in similarly digested pGFP-N-FUS-*SPO20*$^{151\text{-}273}$ (Nakanishi *et al*., 2004). An EcoRI-XhoI fragment carrying the coding region of mRFP-*SPO20*$^{151\text{-}273}$ was then cloned from this construct into pRS426-TEF (Mumberg *et al*., 1995). pKL187PSSP1 is a modified pKL187 (Sanchez-Diaz *et al*., 2004) containing the *SSP1* promoter in place of the *CUP1* promoter. A 700-base pair fragment carrying the *SSP1* promoter was amplified form pRS314-SSP1-HA by using primers SSP1FPromoterMfe1 and SSP1RpromoterEcoR1. The PCR product was digested with Mfe1 and EcoR1 and ligated to the vector backbone of similarly digested pKL187. p926 (gift from A. Amon, Massachusetts Institute of Technology, Cambridge, MA) is pRS306-Pgpd1-GAL4.ER (Benjamin *et al*., 2003), an integrative plasmid containing a GAL4-endoplasmic reticulum (ER) fusion under the control of the *GPD1* promoter. pRS306-AMA1pr-AMA1 was constructed as follows. To remove the sporulation-specific intron (base pairs 1184–1276), a 5′ fragment of *AMA1* open reading frame (ORF) was amplified with primers FAMA1EcoRI (+631) and RNdeI and blunt-end ligated into pBluescript at the EcoRV restriction enzyme site to create pBluescriptAma1A. This was followed by amplification of a 3′ *AMA1* ORF fragment with primers FAMA1Nde1 and RAMA1Pst1stop. This fragment was digested with NdeI and PstI and ligated to similarly digested pBluescriptAma1A. The removal of the intron sequence yielded a conservative amino acid change at position 236 from a cysteine to a serine. This intronless sequence lacks the 5′ end of the coding sequence. To place the full-length *AMA1* sequence under its own promoter, we used overlap polymerase chain reaction (PCR). We amplified a 5′ fragment of *AMA1* by using primers ADO5 and ADO10. This product was mixed with a vector carrying

Table 1. *S. cerevisiae* strains used in this study

Strain	Genotype	Source
AN117-4B	*MATα ura3 leu2 trp1 his3Δsk arg4-NspI lys2 ho::LYS2 rme1::LEU2*	Neiman *et al.* (2000)
AN117-16D	*MAT**a** ura3 leu2 trp1 his3Δsk lys2 ho::LYS2*	Neiman *et al.* (2000)
AN120	Cross of AN117-4B and AN117-16D	Teiman *et al.* (2000)
ADY12	*MAT**a** ura3 leu2 trp1 his3Δsk lys2 ho::LYS2 ama1Δ::CgTRP1*	This study
ADY13	*MATα ura3 leu2 trp1 his3Δsk arg4-NspI lys2 ho::LYS2 rme1::LEU2 ama1Δ::CgTRP1*	This study
ADY64	*MATα ura3 leu2 trp1 his3Δsk arg4-NspI lys2 ho::LYS2 rme1::LEU2 ama1Δ::HIS3*	This study
ADY65	*MAT**a** ura3 leu2 trp1 his3Δsk lys2 ho::LYS2 ama1Δ::HIS3*	This study
ADY66	Cross of ADY64 and ADY65	This study
TC37	*MATα ura3 leu2 trp1 his3Δsk arg4-NspI lys2 ho::LYS2 rme1::LEU2 SSP1::3xHA::his5*	This study
TC38	*MAT**a** ura3 leu2 trp1 his3Δsk lys2 ho::LYS2 SSP1::3xHA::his5*	This study
TC529	Cross of TC37 and TC38	This study
ADY183	*MAT**a** ura3 leu2 trp1 his3Δsk lys2 ho::LYS2 ama1Δ::HIS3 SSP1::3xHA:his5$^+$*	This study
ADY184	*MATα ura3 leu2 trp1 his3Δsk arg4-NspI lys2 ho::LYS2 rme1::LEU2 ama1Δ::HIS3 SSP1::3xHA::his5*	This study
ADY185	Cross of ADY183 and ADY184	This study
ADY183-AMA1	*MAT**a** ura3::AMA1::URA3 leu2 trp1 his3Δsk lys2 ho::LYS2 ama1Δ::HIS3 SSP1::3xHA:his5$^+$*	This study
ADY184-AMA1	*MATα ura3::AMA1::URA3 leu2 trp1 his3Δsk arg4-NspI lys2 ho::LYS2 rme1::LEU2 ama1Δ::HIS3 SSP1::3xHA::his5$^+$*	This study
ADY185	Cross of ADY183-AMA1 and ADY184	This study
ADY186	ADY183-AMA1 × ADY184-AMA1	This study
ADY216	*MATα ura3 leu2 trp1 his3Δsk arg4-NspI lys2 ho::LYS2 rme1::LEU2 ssp1::kan^R::SSP1prDEGRON-SSP1*	This study
ADY217	*MAT**a** ura3 leu2 trp1 his3Δsk lys2 ho::LYS2 ama1Δ::CgTRP1 ssp1::kan^R::SSP1prDEGRON-SSP1*	This study
ADY218	*MATα ura3 leu2 trp1 his3Δsk arg4-NspI lys2 ho::LYS2 rme1::LEU2 ama1Δ::CgTRP1 ssp1::kan^R::SSP1prDEGRON-SSP1*	This study
ADY220	*MAT**a** ura3 leu2 trp1 his3Δsk lys2 ho::LYS2 ssp1::kan^R::SSP1prDEGRON-SSP1*	This study
ADY221	*MATα ura3 leu2 trp1 his3Δsk arg4-NspI lys2 ho::LYS2 rme1::LEU2 ssp1::kan^R::SSP1prDEGRON-SSP1 UBR1::GAL1pr::HA-UBR1::HIS3*	This study
ADY222	*MAT**a** ura3 leu2 trp1 his3Δsk lys2 ho::LYS2 ama1Δ::CgTRP1 ssp1::kan^R::SSP1prDEGRON-SSP1 UBR1::GAL1pr::HA-UBR1::HIS3*	This study
ADY223	*MATα ura3 leu2 trp1 his3Δsk arg4-NspI lys2 ho::LYS2 rme1::LEU2 ama1Δ::CgTRP1 ssp1::kan^R::SSP1prDEGRON-SSP1 UBR1::GAL1pr::HA-UBR1::HIS3*	This study
ADY224	*MAT**a** ura3 leu2 trp1 his3Δsk lys2 ho::LYS2 ssp1::kan^R::SSP1prDEGRON-SSP1 UBR1::GAL1pr::HA-UBR1::HIS3*	This study
ADY225	*MATα ura3::GPD1prGAL4(848)-ER::URA3 leu2 trp1 his3Δsk arg4-NspI lys2 ho::LYS2 rme1::LEU2 ssp1::kan^R::SSP1prDEGRON-SSP1 UBR1::GAL1pr::HA-UBR1::HIS3*	This study
ADY226	*MAT**a** ura3::GPD1prGAL4(848)-ER::URA3 leu2 trp1 his3Δsk lys2 ho::LYS2 ama1Δ::CgTRP1*	This study
ADY227	*MATα ura3::GPD1GAL4(848)-ER::URA3 leu2 trp1 his3Δsk arg4-NspI lys2 ho::LYS2 rme1::LEU2 ama1Δ::CgTRP1 ssp1::kan^R::SSP1prDEGRON-SSP1 UBR1::GAL1pr::HA-UBR1::HIS3*	This study
ADY228	*MAT**a** ura3::GPD1prGAL4(848)-ER::URA3 leu2 trp1 his3Δsk lys2 ho::LYS2 UBR1::GAL1pr::HA-UBR1::HIS3*	This study
ADY229	*MATα ura3 leu2 trp1 his3Δsk arg4-NspI lys2 ho::LYS2 rme1::LEU2 UBR1::GAL1pr::HA-UBR1::HIS3*	This study
ADY230	*MATα ura3::GPD1prGAL4(848)-ER::URA3 leu2 trp1 his3Δsk arg4-NspI lys2 ho::LYS2 rme1::LEU2 UBR1::GAL1pr::HA-UBR1::HIS3*	This study
ADY231	*MAT**a** ura3 leu2 trp1 his3Δsk lys2 ho::LYS2 UBR1::GAL1pr::HA-UBR1::HIS3*	This study
ADY232	*MAT**a** ura3::GPD1prGAL4(848)-ER::URA3 leu2 trp1 his3Δsk lys2 ho::LYS2 UBR1::GAL1pr::HA-UBR1::HIS3*	This study
ADY233	Cross of ADY216 and ADY220	This study
ADY234	Cross of ADY230 and ADY232	This study
ADY235	Cross of ADY225 and ADY228	This study
ADY236	Cross of ADY226 and ADY227	
ADY239	*MAT**a** ura3::GPD1GAL4(848)-ER::URA3 leu2 trp1 his3Δsk lys2 ho::LYS2 ama1Δ::CgTRP1 UBR1::GAL1pr::HA-UBR1::HIS3*	This study
ADY240	*MATα ura3::GPD1GAL4(848)-ER::URA3 leu2 trp1 his3Δsk arg4-NspI lys2 ho::LYS2 rme1::LEU2 ama1Δ::CgTRP1 UBR1::GAL1pr::HA-UBR1::HIS3*	This study
ADY241	Cross of ADY239 and ADY240	
AN390	*MATa/MATα ura3/ura3 trp1/trp1 his3/his3 TEF2::GFP::his5$^+$/TEF2::GFP::his5$^+$*	Coluccio *et al.* (2008)
JSP22	*MAT**a**/MATα ura3/ura3 TRP1/trp1 his3/his3 TEF2::GFP::his5$^+$/TEF2::GFP::his5$^+$ LEU2/leu2Δ0 arg4-NspI/ARG4 ama1Δ::HIS3/ama1Δ::HIS3*	This study
JSP65	*MAT**a** CLB2pr::CDC15::kan^R TEF2::GFP::his5$^+$ arg4-NspI leu2Δ0 ura3 trp1*	This study
JSP64	*MATα CLB2pr::CDC15::kan^R TEF2::GFP::his5$^+$ leu2Δ0 ura3 trp1*	This study
JSP118	Cross of JSP65 × JSP64	This study
JSP89	*MAT**a** CLB2pr::CDC15::kan^R TEF2::GFP::his5$^+$ arg4-NspI leu2Δ0 ura3 trp1 ura3::AMA1::URA3*	This study
JSP88	*MATα CLB2pr::CDC15::kan^R TEF2::GFP::his5$^+$ leu2Δ0 ura3 trp1 ura3::AMA1::URA3*	This study
JSP99	Cross of JSP89and JSP88	This study
JSP78	*MAT**a** CLB2pr::CDC15::kan^R TEF2::GFP::his5$^+$ arg4-NspI leu2Δ0 ura3 trp1 ura3::AMA1-m8::URA3*	This study
JSP77	*MATα CLB2pr::CDC15::kan^R TEF2::GFP::his5$^+$ leu2Δ0 ura3 trp1 ura3::AMA1-m8::URA3*	This study
JSP104	Cross of JSP78 and JSP77	This study

Table 2. Plasmids used in this study

Name	Description	Source
pSB8	*DON1::GFP*	Tachikawa *et al.*, (2001)
pRS426-R20	mRFP-Spo20$^{51–91}$	This study
pRS424-R20	mRFP-Spo20$^{51–91}$	Suda *et al.* (2007)
pKL142	*GAL1pr::HA-UBR1*	Kanemaki *et al.* (2003)
p926	*GPD1prGAL4(848)-ER*	Benjamin *et al.* (2003)
pKL187SSP1pr	*kan^R::SSP1prDEGRON-SSP1*	This study
pRS314-SSP1-HA	*SSP1::3XHA*	This study
pRS306-AMA1pr-AMA1	*AMA1*	This study
pRS306-AMA1pr-AMA1-IA	*AMA1^{R593A}*	This study
pRS306-AMA1pr-AMA1-ΔIR	*AMA1$^{\Delta IR}$*	This study
YIplac128-AMA1	*AMA1*	Oelschlaegel *et al.* (2005)
YIplac128-AMA1-m8	*AMA1-m8*	Oelschlaegel *et al.* (2005)

the intronless *AMA1* 3′ sequence and amplified with primers ADO3 and ADO5, which yielded a 2-kb DNA fragment. Separately, oligos PAMA1F and PAMA1R were used to amplify 500 base pairs of the upstream sequence of the *AMA1* gene, and this promoter region was cloned into the XhoI and Kpn1 sites of pRS306 to create pRS306-AMA1pr. The full-length intronless *AMA1* ORF was then inserted into a pRS306-AMA1pr, at the XhoI and SpeI sites creating plasmid pRS306-AMA1pr-AMA1. The *AMA1* in this plasmid was shown to be functional based on its ability to complement the *ama1*Δ*/ama1*Δ phenotype (data not shown). Plasmids pRS306-AMA1pr-AMA1-IA and pRS306-AMA1pr-AMA1-ΔIR were constructed by reamplifying the intronless AMA1 ORF by using the oligo pairs Ama1pFXhoI and Ama1StopIA, or Ama1pFXhoI and Ama1StopΔIR, respectively. The Ama1StopIA and Ama1StopΔIR oligos incorporate the mutations at the extreme C terminus of the coding region. The PCR fragments carrying the mutant alleles were then cloned into pRS306-AMA1-pr as XhoI-SpeI fragments. pRS426-AMA1pr-AMA1-ΔIR was created by moving a KpnI and SpeI fragment carrying the gene from pRS306-AMA1pr-AMA1-ΔIR into pRS426 (Christianson *et al.*, 1992).

Sporulation Assays

Cells were sporulated in liquid medium as described previously (Neiman, 1998). Briefly, strains were grown at 30°C overnight in YPD or in selective medium if they contained plasmids. The cultures were then diluted to a cell density of 0.2 at OD_{660} in YP media containing 2% potassium acetate and incubated at 30°C overnight. Cells were then washed once in distilled water and then resuspended in sporulation medium (2% potassium acetate) at a cell density of 1.2 at OD_{660}, and these cultures were incubated at 30°C. For experiments using the degronSSP1, 25 nM β-estradiol (Sigma-Aldrich, St. Louis, MO) was added to the sporulating cells at the time of transfer to sporulation medium. Cells were cultured at 23°C for 2 h and then moved to restrictive temperature.

Ether Tests

Cells were sporulated at permissive (25°C) and restrictive (35°C) temperatures for the degron cassette in the presence or absence of 25 nM β-estradiol (Sigma-Aldrich). Serial dilutions of sporulated cells from each culture condition were spotted onto two duplicate YPD plates, and one plate was exposed to ether vapor for 5 min by inversion over an ether-soaked paper filter. Plates were photographed after incubation at 30°C for 1 d.

Immunoblotting and Immunofluorescence

For the Western analysis of Ssp1, cell extracts were prepared as described previously (Moreno-Borchart *et al.*, 2001). Briefly, cells were lysed, and proteins were separated by SDS-polyacrylamide gel electrophoresis (PAGE) and transferred onto nitrocellulose. Ssp1 was detected using anti-HA antibody 12CA5 (Roche Diagnostics, Indianapolis, IN) at 1 μg/ml. Monclonal anti-porin (Invitrogen, Carlsbad, CA) and polyclonal goat anti-Clb5 antibodies (Santa Cruz Biotechnology, Santa Cruz, CA) were also used at 1 μg/ml. For detection, the secondary antibody IR Dye 680 goat anti-mouse (LI-COR Biosciences, Lincoln, NE) and donkey anti-goat antibodies conjugated to IR Dye 800 were used at 1:10,000 dilutions of 0.5 mg/ml stocks. Membranes were scanned using Odyssey Infrared Imaging system (LI-COR Biosciences), and the signal intensities for all three proteins measured (Ssp1 and porin were measured on the same membrane, Clb5 from a separate membrane with equal volumes of each sample loaded). To allow comparison of levels between wild-type and *ama1*Δ cells, the porin signals in each lane were normalized to the value in the wild-type time zero lane and then the Ssp1 and Clb5 intensities at each time point were normalized to the porin signal at that same time point. Indirect immunofluorescence of the β-glucan layer was performed as described previously (Tachikawa *et al.*, 2001).

Time-Lapse Fluorescence Microscopy

Time-lapse imaging was done as follows. Sporulation media containing 1.5% agarose-S was dropped on the glass surface of a glass-bottomed dish. Solidified media were removed from dish, and cells were spotted on a flat surface of media, put again on a dish to sandwich cells between glass and media. Images were captured on an Axiovert 100 microscope (Carl Zeiss, Thornwood, NY) at 2-min intervals for wild type and at 4-min intervals for the *ama1*Δ mutant by using of IPLab 3.6.5a software (Scanalytics, Rockville, MD). At each time point, 12 Z-sections were collected at 0.5-μm intervals. The temperature was kept at 28°C. Deconvolution was performed using an EPR system (Scanalytics) and three-dimensional stacks using IPLab 3.6.5a.

Fluorescence Loss in Photobleaching (FLIP) Assays

For FLIP microscopy, strains AN390 and JSP22 were first transformed with pRS424-R20 and pRS426-R20, respectively. A thin layer of 1.5% agarose containing 1% potassium acetate and 2 mM $NaHCO_3$ was prepared. A 1.5-cm square of this agarose was cut out, and sporulated cells were spotted onto this square. The agarose square was then placed cell-side down onto a glass-bottomed Petri dish (MatTek, Ashland, MA), and cells were observed on an LSM 510 inverted microscope (Carl Zeiss).

For photobleaching, a 488-nm argon laser was used at 100% power. A cytoplasmic area was photobleached for 8 s with 75 pulses per bleaching. To analyze fluorescence intensity, LSM 510 META software version 3.2 (Carl Zeiss) was used.

For the FLIP assay, cells displaying mRFP-Spo20$^{51-91}$ fluorescence (a prospore membrane marker) were selected. An area of the mother cell cytoplasm outside of the prospore membrane was photobleached four times over a period of 14 min, and the GFP fluorescence of Tef2-GFP was monitored every 15 s. Using the software, the fluorescence intensities were then measured in several areas in the cell: 1) the site of bleaching in the cytoplasm, 2) a cytoplasmic area separate from the bleached area and outside of the prospore membrane, 3) an area inside the prospore membrane, and 4) an area of cytoplasm in an unbleached, neighboring cell.

RESULTS

The Leading Edge Complex Persists in ama1Δ Mutants

Time-lapse videomicroscopy was used to examine the growth of the prospore membrane in wild-type cells using a fusion of RFP to the lipid binding domain of Spo20 to visualize the membranes (Nakanishi *et al.*, 2004). These studies demonstrated that as prospore membranes expanded they progressed through a series of discrete morphological stages (Figure 1 and Supplemental Movie 1). They began as small horseshoe-shaped structures that expanded into small round structures and initially maintained that round shape as they expanded. As meiosis II progressed, the membranes elongated into a tubular shape. After extending as tubes, the membranes widened in the middle to form an oval before a rapid transition back to a round shape. This final change in shape may correspond to the closure of the prospore membrane.

To examine the relationship between morphological change and closure, a Don1-GFP fusion was used to examine

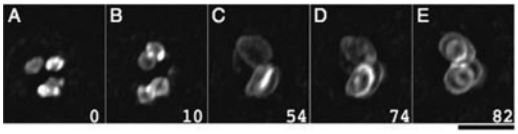

Figure 1. Morphological changes of the prospore membrane in wild-type cells. AN120 containing pRS424-G20 (GFP-Spo20$^{51-91}$) was sporulated and examined by fluorescence microscopy. Five different morphologies were observed in the following temporal order: a horseshoe shape (A), a small circular shape (B), a tubular shape (C), an oval shape (D), and a sphere shape (E). Images shown are frames from a video of prospore membrane formation of a single cell. Each image is a projection through a deconvolved image stack. The numbers indicate the time elapsed, in minutes, from the image captured in A. The entire movie is available as Supplemental Video 1. Bar, 5 μm.

the leading edge protein complex in parallel with membrane growth. The movies revealed that disassembly of the leading edge ring, as seen by dispersal of Don1-GFP fluorescence, happens a few minutes before the final rounding up of the prospore membrane (Figure 2A and Supplemental Movie 2). Removal of the core leading edge protein Ssp1 from the leading edge has been proposed to be required for prospore membrane closure (Maier *et al*., 2007), consistent with the idea that the rounding up of the membrane correlates with cytokinesis.

When *ama1*Δ mutants were examined in the same way, different behaviors of the prospore membrane and Don1-GFP were seen. Membrane expansion was initially normal, but the duration of the tubular phase was greatly extended (Figure 2B and Supplemental Movie 3). Moreover, even

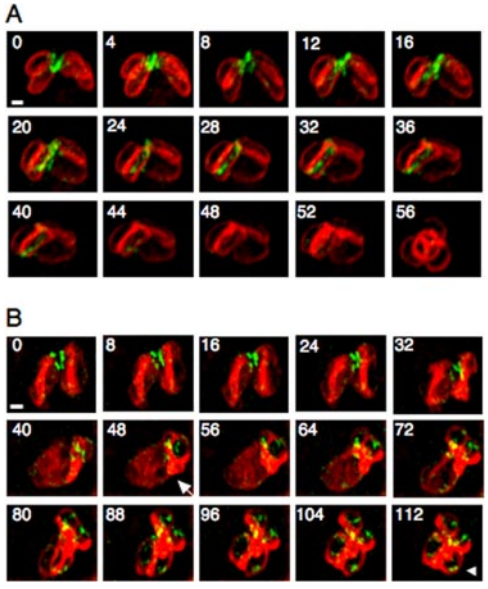

Figure 2. Time-lapse analysis of prospore membranes and the leading edge complex in late meiosis II. (A) AN120 (wild-type) carrying pRS424-R20 (RFP-Spo20$^{51-91}$) and pSB8 (Don1-GFP) was cultured on sporulation media for 7 h and analyzed by time-lapse fluorescence microscopy. Numbers indicate minutes elapsed from start of observation. The entire movie is available as Supplemental Video 2. Bar, 1 μm. (B) ADY66 (*ama1*Δ/*ama1*Δ) carrying pRS424-R20 and pSB8 was cultured on sporulation media for 10 h and analyzed by time-lapse fluorescence microscopy. Numbers indicate minutes elapsed from start of observation. Arrow at 48 min indicates a site of abnormal prospore membrane growth. Arrowhead at 112 min indicates an intact Don1-GFP ring. The entire movie is available as Supplemental Video 3. Bar, 1 μm.

though in many cells the membranes eventually rounded up, the Don1-GFP staining never dispersed as in wild type. Rather, discrete foci of Don1-GFP fluorescence, and occasionally intact rings, persisted throughout the time course. At later times, abnormal prospore membrane structures began to accumulate in the mutant. Don1 localization is dependent on Ssp1 (Moreno-Borchart *et al*., 2001). Therefore, Don1-GFP serves as a marker for Ssp1 localization in these cells. If disassembly of the leading edge complex and rounding up of the prospore membrane are linked to closure, these observations suggest that cytokinesis may be defective in the *ama1*Δ mutant.

*FLIP Assay for Closure Reveals a Defect in ama1*Δ *Mutants*

To directly assess whether *AMA1* has a role in cytokinesis, we developed a FLIP assay for membrane closure based on the ability of a GFP-tagged protein to diffuse between the presumptive ascal and spore cytoplasms. A strain expressing both a GFP-tagged *TEF2* gene, encoding translation elongation factor 2, as well as mRFP-Spo20$^{51-91}$ was sporulated. During meiosis II a small region of the cytoplasm outside of the prospore membranes was repeatedly photobleached with pulses from a laser and the fluorescence intensity of the Tef2-GFP signal at spots both inside and outside of the prospore membranes was monitored over time (Figure 3A). Cells were examined at different stages of prospore membrane growth, as defined by the shape and size of the membrane.

In wild-type cells with small round or tubular prospore membranes, photobleaching of a spot outside of the prospore membrane led to loss of GFP fluorescence throughout the entire cell, indicating that the Tef2-GFP protein was free to diffuse between cytoplasm located inside and outside of the prospore membrane (Table 3 and Figure 3A). However in cells where the prospore membrane had made the transition from tubular to oval or round shaped, GFP fluorescence within the prospore membrane was no longer sensitive to photobleaching in the cytoplasm outside of the prospore membrane (Table 3 and Figure 3A). Thus, the change in prospore membrane shape correlates precisely with the separation of the mother cell cytoplasm into distinct ascal and prospore compartments. In combination with the video microscopy, these results also provide additional evidence that disassembly of the leading edge complex is correlated with cytokinesis.

This FLIP assay was then used to examine membrane closure in the *ama1*Δ mutant. As in wild-type cells, Tef2-GFP diffused freely throughout the cytoplasm in *ama1*Δ cells with small or tubular prospore membranes (Figure 3B). However, in *ama1*Δ cells only ~30% of the round or oval prospore membranes were closed off to the ascal cytoplasm (Table 3 and Figure 3B). At least half of the membranes examined clearly remained open. The remaining 20% gave ambiguous results, in which loss of fluorescence due to photobleaching was intermediate between the obviously open or closed membranes. This may represent cells where closure is incomplete, leaving a small diffusion-limiting opening, or simply be a result of the technical difficulty of photobleaching the ascal cytoplasm alone in cells with abnormal prospore membranes. That some of the prospore membranes do close suggests either that there may be an *AMA1*-independent means of removing the leading edge complex, for example by some functional overlap with *CDC20*, or possibly an alternative pathway to membrane closure. Nonetheless, the abundance of open prospore membranes demonstrates that *ama1*Δ mutants are defective in the cytokinesis at the end of meiosis II.

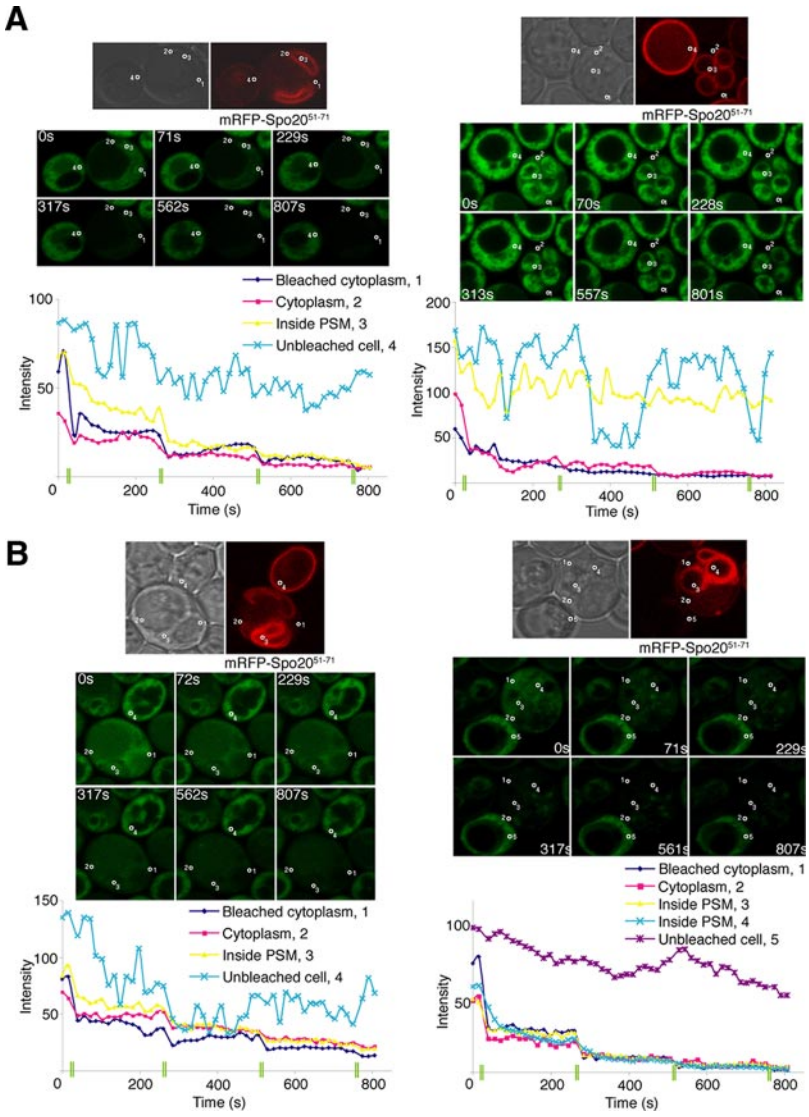

Figure 3. Morphological change of the prospore membrane coincides with prospore membrane closure. Wild-type (AN390) and *ama1*Δ (JSP22) cells carrying containing pRS424-R20 (RFP-Spo20$^{51-91}$) were cultured and prepared for the FLIP assay as described in *Materials and Methods*. The prospore membranes were visualized with mRFP-Spo20$^{51-91}$. The diffuse cytoplasmic fluorescence is from Tef2-GFP. (A) Time-lapse series of FLIP assay in wild-type cells. Circle 1 indicates the region of the ascal cytoplasm that was photobleached. Circle 2 indicates a region ascal cytoplasm opposite to the bleached area. Circle 3 indicates the cytoplasm inside a prospore membrane. Circle 4 indicates the cytoplasm of a nonbleached neighboring cell. Fluorescence intensity dropped throughout the cell containing "tubular"-shaped prospore membranes (left). Fluorescence intensity dropped only in the ascal cytoplasm of a cell containing sphere-shaped prospore membranes (right). (B) Time-lapse series of FLIP assay in *ama1*Δ cells. Circle 1 indicates the region of the ascal cytoplasm that was photobleached. Circle 2 indicates a region ascal cytoplasm opposite to the bleached area. Circle 3 indicates the cytoplasm inside a prospore membrane. Circle 4 indicates the cytoplasm of a nonbleached neighboring cell. Fluorescence intensity decreased throughout the cell in cells displaying both tubular (left) and sphere (right) phase prospore membranes. Graphs display quantitation of fluorescence intensity at each monitored spot throughout the course of the assay. Vertical green lines on the *x*-axis indicate the times at which laser pulses were used to induce photobleaching.

Ssp1 Protein Levels Persist in the ama1Δ Mutant

Our microscopy results indicate that *ama1*Δ mutants are defective both in prospore membrane closure and in disassembly of the leading edge complex. The leading edge component Ssp1 has been shown to antagonize membrane fusion when expressed in vegetative cells leading to the suggestion that closure of the prospore membrane requires removal of Ssp1 from the leading edge (Maier *et al.*, 2007). In

Table 3. Assay of prospore membrane closure by FLIP in wild-type and *ama1* cells

	Membrane class[b]			
		% oval or spherical		
Relevant genotype[a]	% horseshoe, small circular, or tubular Closed	Closed	Open	Ind.[c]
Wild type	0 (0/98)	100 (91/91)	0 (0/91)	0 (0/91)
*ama1*Δ/*ama1*Δ	N.T.[d]	31 (17/55)	53 (29/55)	16 (9/55)

[a] Strains used in these experiments are AN390 (wild type) and JSP22 (*ama1*Δ/*ama1*Δ) transformed with pRS426-R20.
[b] FLIP assay was performed to measure loss or retention of fluorescence inside prospore membranes in each of the morphological classes displayed in Fig. 1.
[c] Indeterminate: fluorescence signal inside the prospore membrane displayed a modest response to photobleaching of the ascal cytoplasm.
[d] N.T., not tested.

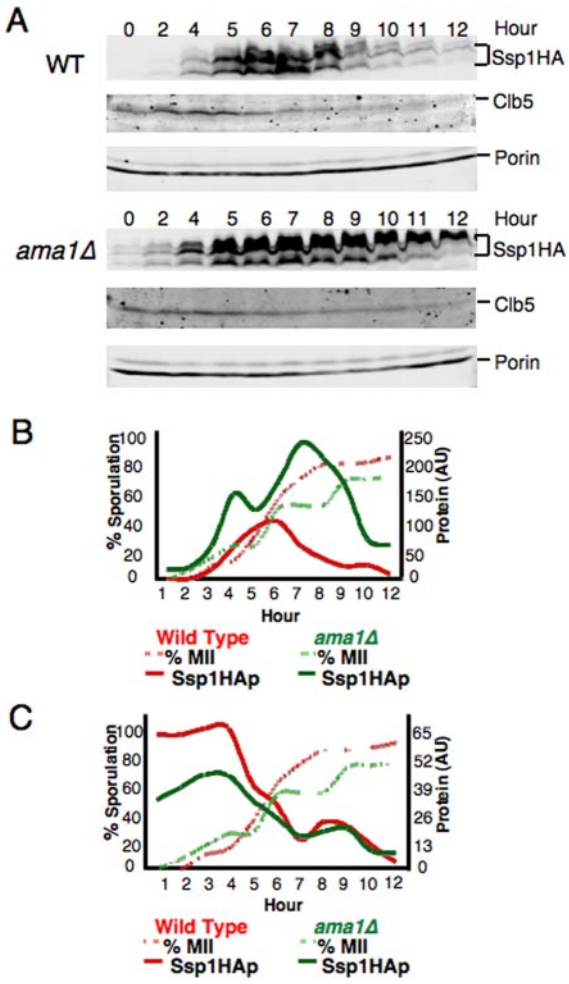

Figure 4. Ssp1p is degraded in an APC^{AMA1}-dependent manner. (A) Western analysis of Ssp1 protein levels. WT and *ama1*Δ strains were sporulated and aliquots removed at specific time points both to monitor nuclear divisions and prepare samples for SDS-PAGE. Extracts were examined for the presence of Ssp1-HA, indicated with brackets, detected by anti-HA antibody as well as Clb5 and the mitochondrial porin protein. (B and C) Quantitation of levels of Ssp1HA and Clb5 proteins during the sporulation time course shown in A. Dashed lines indicate percentage of cells having completed meiosis II at each time point. Solid lines indicate levels of Ssp1-HA and Clb5 proteins in arbitrary units. Levels of Ssp1-HA and Clb5 were determined by normalization against the levels of the mitochondrial porin at each time point.

this light, one simple explanation for our results would be that APC^{Ama1} promotes degradation of Ssp1 and this degradation allows prospore membrane closure.

To determine whether *AMA1* influences the stability of the Ssp1 protein, the levels of a HA-tagged Ssp1 protein were examined across sporulation time courses in wild-type and *ama1*Δ strains (Figure 4). To correlate protein levels with the events of meiosis, cells were also fixed at each time point, stained with DAPI, and the nuclear morphology was examined in the fluorescence microscope. In wild-type cells, Ssp1 protein began to accumulate after 3 h in sporulation medium, coincident with the onset of the meiotic divisions. Consistent with earlier reports (Maier *et al*., 2007), Ssp1 levels peaked after 6 h and then fell sharply as the population reached the end of meiosis. By contrast, in the *ama1*Δ cells, Ssp1 levels increased as in wild type, but the protein accumulated to a much greater extent than in wild-type cells. At later time points, after the bulk of cells in the population had completed meiosis II, Ssp1 levels declined in the *ama1*Δ mutant strain, but even after 12 h the level of Ssp1 was comparable with the peak level in wild-type cells. Thus, although some degradation of Ssp1 is seen, loss of *AMA1* leads to an accumulation and a persistence of the Ssp1 protein at the end of meiosis (Figure 4B).

Because *ama1*Δ mutants have been reported to have defects in meiotic progression in some backgrounds (Cooper *et al*., 2000), it was possible that this accumulation and persistence of Ssp1 was an indirect consequence of a meiotic defect in the *ama1*Δ strain. To examine this possibility, we also measured the abundance of Clb5, a protein degraded at the completion of meiosis II (Carlile and Amon, 2008), in the two strains (Figure 4C). The levels of Clb5 in both strains were comparable throughout the time course, indicating that the accumulation of Ssp1 is not a consequence of a more general defect in protein turnover at the end of meiosis II in the *ama1*Δ mutant.

The ama1Δ Sporulation Defect Can Be Partially Rescued by a Conditional SSP1

If *AMA1*-mediated turnover of Ssp1 is required for prospore membrane closure and this cytokinesis defect is responsible for the subsequent spore wall formation phenotypes of *ama1*Δ, then mutation of *SSP1* might be expected to rescue the *ama1*Δ sporulation defect. Because *SSP1* is essential for proper prospore membrane assembly, a conditional allele of *SSP1* is required so that Ssp1 protein can be inactivated after prospore membranes have formed and expanded. A point mutation creating a conditional allele of *SSP1* has been reported previously (Esposito *et al*., 1970; Maier *et al*., 2007), but in our strain background the phenotype of this mutant was very mild, and no restoration of sporulation was observed when it was combined with *ama1*Δ (Diamond, unpublished observations). We therefore sought to engineer a conditional allele of *SSP1* by using a degron cassette (Sanchez-Diaz *et al*., 2004). Fusion of one copy of ubiquitin followed by a temperature-sensitive form of dihydrofolate reductase (DHFR) to the amino terminus of a heterologous protein can be used to generate proteins whose stability is temperature dependent in vivo (Sanchez-Diaz *et al*., 2004). Cleavage of the ubiquitin moiety reveals an amino-terminal arginine residue on the $DHFR^{ts}$ and, upon shift to elevated temperature, the $DHFR^{ts}$ fusion protein is degraded by the N-end rule pathway. Efficient turnover in this system also requires overexpression of the ubiquitin ligase Ubr1 (Sanchez-Diaz *et al*., 2004). To induce Ubr1 in our strains, both a *GAL* promoter driven *UBR1* and a plasmid expressing a fusion of the Gal4 transcription factor to the hormone-binding domain of the human estrogen receptor were integrated into the genome. This Gal4 fusion can induce transcription only in the presence of steroid ligands such as β-estradiol (Picard, 1999). A strain expressing the fusion form of *SSP1* (hereafter *degssp1*) as its only source of Ssp1 and carrying the *GAL-UBR1* and Gal4-ER plasmids displays conditional sporulation; sporulation is blocked only in the presence of both estradiol, to induce *UBR1*, and elevated temperature to destabilize Ssp1 (Figure 5A).

The *degssp1* allele was then combined with a deletion of *AMA1*. Cells were sporulated in the presence of β-estradiol at 23°C for 2 h to allow them to enter sporulation and then shifted to 35°C and incubated overnight. Sporulation was assayed both by ether test (Figure 5B) and by direct examination in the light microscope (Figure 5C). Under this regimen, wild-type cells displayed good sporulation at both

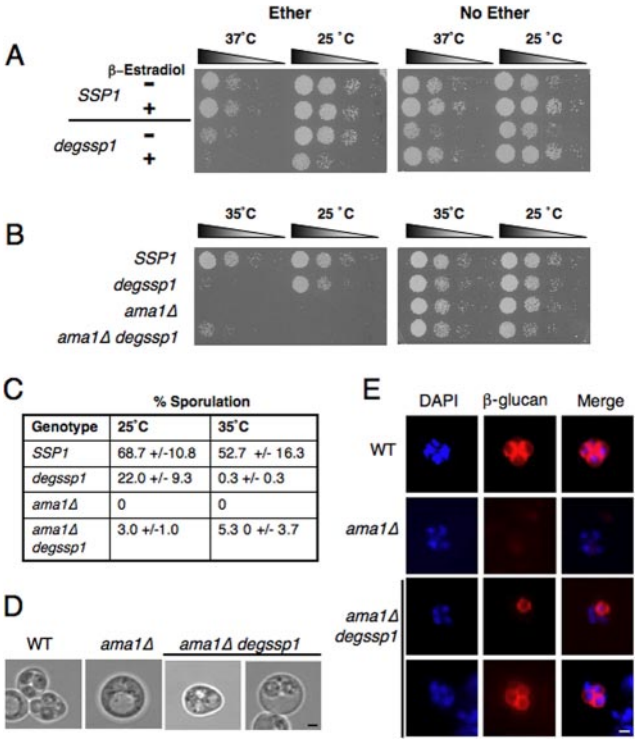

Figure 5. Premature degradation of Ssp1 suppresses the *ama1*Δ phenotype. (A) *degssp1* is a conditional allele of *SSP1*. Wild-type (ADY234) or *degssp1* (ADY235) strains carrying *GAL1::UBR1* were sporulated at permissive temperature (25°C) and restrictive temperature (37°C) in the presence or absence of 25 nM β-estradiol. Serial dilutions of cells in each culture condition were spotted onto YPD plates and cells in the left panel were exposed to ether vapor to kill unsporulated cells. Growth indicates the presence of spores. (B) Inactivation of *SSP1* suppresses the *ama1*Δ phenotype. Wild-type (ADY234) *degssp1* (ADY235), *ama1*Δ (ADY236), and *ama1*Δ *degssp1* (ADY241) strains carrying *GAL1::UBR1* were sporulated at permissive temperature in the presence of β-estradiol. Samples were transferred at 2 h to restrictive temperature (35°C) and incubated overnight. Serial dilutions of cells in each culture condition were spotted onto YPD plates and subsequently exposed to ether vapor. (C) Quantitation of *degssp1* suppression of *ama1*Δ. Strains were sporulated as described in B, and percentage of sporulation was determined in each culture by light microscopy. Asci containing one to four visible spores were all scored as sporulated. Average values from three separate experiments are given. (D) DIC images of WT (ADY234), *ama1*Δ (ADY241), and *degssp1 ama1*Δ (ADY236) strains sporulated at restrictive temperature (35°C) in the presence of β-estradiol. (E) Anti-β-glucan staining of asci of the same strains shown in A. Chromatin is visualized by staining with DAPI (blue). Bar, 2 μm.

temperatures, an *ama1*Δ strain failed to produce spores at either temperature, and the *degssp1* strain displayed temperature-sensitive sporulation. By contrast, the *ama1*Δ *degssp1* strain displayed very weak sporulation at low temperature that was markedly improved by raising the temperature to 35°C. Tests of different temperature regimes and incubation times before temperature upshift indicated that the protocol used in these experiments provided the best level of sporulation in the double mutant (Diamond, unpublished observations). Although this level of sporulation was only ~10% of the wild type, no spores are ever seen in the *ama1*Δ mutant alone. Thus, this represents a significant suppression of *ama1*Δ by *degssp1*. Reproducibly, at 35°C, slightly higher sporulation was seen in the *ama1*Δ *degssp1* strain than in the strain carrying *degssp1* alone (Figure 5C). Thus, reciprocally, deletion of *AMA1* improves sporulation of *degssp1* cells. The accumulation of Ssp1-HA seen in *ama1*Δ mutants (Figure 4) suggests that this improvement of *degssp1* sporulation may be due to stabilization of degSsp1 that has escaped from N-end rule mediated degradation.

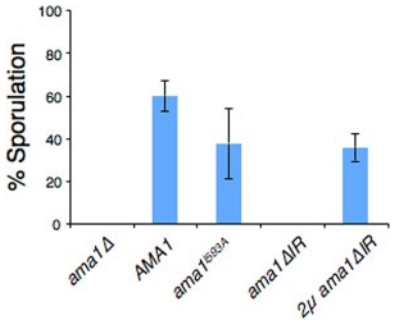

Figure 6. The carboxy-terminal APC interaction motif is essential for Ama1 function. An *ama1*Δ strain (ADY66) was transformed with the indicated *AMA1* alleles and sporulation efficiency was assessed by light microscopy. Averages are calculated from five separate experiments. Bars indicate 1 SD from the mean.

When *ama1*Δ cells are sporulated they fail to synthesize spore wall components. As spore wall assembly is required for the generation of visible spores, the incomplete rescue of *ama1*Δ by *degssp1* could represent strong suppression of the cytokinesis defect masked by a subsequent spore wall synthesis phenotype. To address this possibility, spore wall synthesis in the *ama1*Δ *degssp1* mutant was examined using anti-β-1,3-glucan antibodies (Figure 5E). Examination of anti-β-1,3-glucan staining in the mutant demonstrated that the number of β-1,3-glucan containing prospores varied between asci. The distribution of β-glucan staining was comparable with the distribution of visible spores as seen in differential interference contrast microscopy (DIC) (Diamond, unpublished observations). Because β-glucan deposition is required for acquisition of refractility and occurs early in spore wall formation (Tachikawa *et al.*, 2001; Coluccio *et al.*, 2004), this result suggests that those prospores that bypass the cytokinesis block in the *ama1*Δ *degssp1* strain go on to complete spore wall synthesis.

A Motif Important for Interaction with the APC Is Essential for Ama1 Function

Cdc20/Fizzy family members carry two motifs, a C-box and a carboxy-terminal isoleucine and arginine (IR) that are important for interaction with the APC (Schwab *et al.*, 2001; Vodermaier *et al.*, 2003). The IR motif has been shown to bind to the APC subunit Cdc27, and mutation of the IR motif in Cdh1 or Cdc20 blocks their interaction with the APC in vitro and inactivates Cdh1 in vivo (Vodermaier *et al.*, 2003; Kraft *et al.*, 2005; Oelschlaegel *et al.*, 2005). Similarly, mutation of the carboxy-terminal arginine residue of Ama1 to an alanine blocks its ability to interact with the APC in vitro (Oelschlaegel *et al.*, 2005). We examined the phenotype of this arginine to alanine mutation ($AMA1^{R593A}$) in vivo. Despite the strong effect of this mutation in vitro, cells expressing $AMA1^{R593A}$ from the chromosome as the only form of *AMA1* showed only a mild sporulation defect (Figure 6). By contrast, deletion of both the carboxy-terminal isoleucine and arginine residues (*IR*Δ) strongly reduced sporulation. When this $AMA1^{IR}\Delta$ allele was overexpressed from a high copy plasmid, the mutant was able to partially rescue the

Table 4. Suppression of the Clb2pr-Cdc15 closure defect by Ama1-m8

	% oval or spherical prospore membranes		
Relevant genotype[a]	Closed	Open	Ind.[b]
CLB2pr::CDC15	53 (27/51)	23.5 (12/51)	23.5 (12/51)
CLB2pr::CDC15 ura3::AMA1	45 (23/51)	49 (25/51)	6 (3/51)
CLB2pr::CDC15 ura3::AMA1-m8	80 (41/51)	14 (7/51)	6 (3/51)

[a] Strains used in these experiments are JSP118 (wild type) and JSP99 (*CLB2pr::CDC15 ura3::AMA1*) and JSP104 (*CLB2pr::CDC15 ura3::AMA1-m8*) transformed with pRS424-R20.

[b] Indeterminate: fluorescence signal inside the prospore membrane displayed a modest response to photobleaching of the ascal cytoplasm.

sporulation defect of *ama1*Δ. These observations demonstrate that the carboxy-terminal IR motif is important, although not essential, for Ama1 function in vivo. This suggests that interaction with APC is necessary for Ama1 to promote sporulation but that, in contrast to the in vitro studies, in vivo the IR motif enhances but is not absolutely required for this interaction.

An Activated Form of Ama1 Can Promote Cytokinesis in a Meiotic Exit-defective Mutant

The protein kinase Cdc15 is a component of a pathway, the MEN, that is required for completion of mitosis in vegetative cells. Cdc15 protein can be depleted from sporulating cells by placing the gene under control of the sporulation-repressed *CLB2* promoter (Kamieniecki *et al*., 2005; Pablo-Hernando *et al*., 2007). Although homozygous *CLB2pr-CDC15* cells progress through meiosis with normal kinetics, the cells fail to form spores and display other phenotypes, including defective spindle disassembly, that suggest a failure to properly exit from meiosis II (Pablo-Hernando *et al*., 2007).

APC^{Ama1} activity is inhibited during meiosis by both the Mnd2 subunit of APC and by Clb-Cdc28 kinase and both of these antagonistic activities are down-regulated as cells complete meiosis (Dahmann and Futcher, 1995; Oelschlaegel *et al*., 2005; Carlile and Amon, 2008). If, as a consequence of the failure to exit meiosis properly, a *CLB2pr-CDC15* mutant does not release the inhibition of APC^{Ama1}, we would expect to find a prospore membrane closure defect in these cells. To test this possibility, we used the FLIP assay to examine prospore membrane closure in a *CLB2pr-CDC15* strain. As reported previously (Pablo-Hernando *et al*., 2007), the *CLB2pr-CDC15* cells displayed a prospore membrane growth defect, with many cells displaying only one or two membranes that are full size by the end of meiosis II. Because small membranes are usually open in wild-type cells, we limited our analysis of closure to the largest membrane in each cell. In the *CLB2pr-CDC15* strain, 53% of these membranes were closed and 24% were open, with the remaining membranes in the indeterminate class (Table 4). Thus, depletion of Cdc15 results in a prospore membrane closure defect.

If the closure defect in *CLB2pr-CDC15* cells is due to inhibition of APC^{Ama1}, then relief of this inhibition should restore prospore membrane closure in the mutant. Combining a deletion of *MND2* with *CLB2pr-CDC15* is problematic because unregulated APC^{Ama1} activity in the *mnd2* strain results in defects early in meiosis (Oelschlaegel *et al*., 2005; Penkner *et al*., 2005). By contrast, mutation of eight consensus Cdc28 phosphorylation sites in the Ama1 protein to alanines ($Ama1^{m8}$) does not cause any obvious phenotype (Oelschlaegel *et al*., 2005). We therefore integrated either *AMA1* or *AMA1-m8* into the *CLB2pr-CDC15* strain and examined prospore membrane closure by using the FLIP assay.

Integration of an extra two copies of *AMA1* into these cells did not significantly alter the fraction of prospore membranes that were closed. However, introduction of the *AMA1-m8* allele, increased the fraction of membranes that close in the *CLB2pr-CDC15* cells to 80%. Although modest, a chi-square test indicates that the fraction of closed prospore membranes in the presence of *AMA1-m8* is significantly different from either of the other two strains ($p < 0.001$). These results indicate that the closure defect in the *CLB2pr-CDC15* cells is caused by a failure to activate APC^{Ama1} possibly due to direct phosphorylation of Ama1 by the Cdc28 kinase.

In addition to the prospore membrane closure defect, *CLB2pr-CDC15* cells display defects in prospore membrane growth, meiotic spindle disassembly, and fail to form spores (Pablo-Hernando *et al*., 2007). Expression of *AMA1-m8* did not rescue any of these other phenotypes (Suda and Park, unpublished observations). Thus, the lack of APC^{Ama1} activity is responsible only for the closure defect in these cells.

DISCUSSION

Studies of the leading edge component Ssp1 have demonstrated that the protein is degraded at around the time of prospore membrane closure and that failure to degrade the protein blocks spore formation (Maier *et al*., 2007). Using a FLIP assay, we provide direct evidence that the morphological changes in the prospore membrane that correlate with removal of the leading edge complex are coincident with closure of the prospore membrane. In an *ama1*Δ mutant, Ssp1 degradation and leading edge complex disassembly is delayed and cytokinesis is impaired. This provides direct support for the idea that removal of Ssp1 from the leading edge is required for membrane closure (Maier *et al*., 2007).

A conserved IR dipeptide at the extreme amino terminus is a hallmark of Cdc20/Fizzy proteins (Vodermaier *et al*., 2003). However, the effects of mutations in this motif vary in vivo. Deletion of this motif in the yeast Cdh1 creates a null allele (Kraft *et al*., 2005), whereas cells carrying a deletion of the IR residues of Cdc20 are viable, with only modest effects on function of the protein (Thornton *et al*., 2006). Ama1 falls between these extremes. Deletion of the IR tail does greatly reduce sporulation, but overexpression of this allele can restore activity. The differences between these different APC targeting subunits in sensitivity to carboxy-terminal mutations suggest that in addition to the conserved C-box and IR motifs they may each make unique contacts with the APC that effect the relative importance of the conserved motifs.

Activity of APC^{Ama1} is regulated by both the Mnd2 subunit of the APC and Clb-Cdc28 kinase activity (Oelschlaegel *et al*., 2005; Penkner *et al*., 2005). In the presence of Mnd2, Ama1 cannot promote ubiquitylation of substrates either in vivo or in vitro (Oelschlaegel *et al*., 2005). The Mnd2 protein, however, dissociates from the APC during anaphase II, suggesting that the activity of APC^{Ama1} might be up-regulated at that time (Oelschlaegel *et al*., 2005). Similarly, Clb-Cdc28 kinase activity down-regulates APC^{Ama1} and Clb-Cdc28 kinase activity drops at the end of meiosis II (Dahmann and

Futcher, 1995; Oelschlaegel *et al*., 2005; Carlile and Amon, 2008). Our finding that mutation of the consensus Cdc28 phosphorylation sites of Ama1 allows prospore membrane closure in the *CLB2pr-CDC15* mutant suggests that Cdc28 directly phosphorylates Ama1. Relief of these two different inhibitions might trigger APC^{Ama1} activity at the end of meiosis. This is analogous to the manner in which APC^{Cdh1} activity in mitotic cells is restricted until anaphase by the combination of Cdc28 phosphorylation of Cdh1 and the binding of the APC^{Cdh1} inhibitor Acm1 (Zachariae *et al*., 1998; Martinez *et al*., 2006; Ostapenko *et al*., 2008).

In the case of Cdh1, phosphorylation seems to be the predominant brake on APC^{Cdh1} activity, as mutation of the phosphorylation sites creates a constitutively active, lethal allele (Zachariae *et al*., 1998). By contrast, though we provide evidence that mutation of the sites in Ama1 results in an allele that is dominantly active late in meiosis, in an otherwise wild type cell, the *AMA1-m8* mutant does not produce a phenotype (Oelschlaegel *et al*., 2005). Mutation of *MND2*, however, is sufficient to activate APC^{Ama1} (Oelschlaegel *et al*., 2005; Penkner *et al*., 2005). One interpretation of these observations is that *MND2* provides the primary restraint on APC^{Ama1} activity early in meiosis and that inhibition by Clb-kinase late in meiosis, as Mnd2 activity is lost, allows the activation of APC^{Ama1} to be timed more precisely to exit from meiosis II. In light of the report that different Clb-Cdc28 complexes are active at different times of meiosis (Carlile and Amon, 2008), it will be of interest to determine if APC^{Ama1} is subject to down-regulation by Clb-kinases generally or only those that are active during meiosis II.

Our finding that depletion of Cdc15 results in a cytokinesis defect that can be relieved by a nonphosphorylatable allele of *AMA1* is consistent with the idea that completion of meiosis leads to activation of APC^{Ama1}. These observations, and previous work indicating that removal of Ssp1 from the prospore membrane is important for prospore membrane closure (Maier *et al*., 2007) suggest a model in which Ama1 functions to coordinate exit from meiosis II with cytokinesis. The disappearance of Mnd2 and Clb-Cdc28 kinase activity at the end of meiosis activates APC^{Ama1} leading to the destruction of Ssp1 and disassembly of the leading edge complex. The removal of Ssp1 then allows the prospore membrane to close (Figure 7).

One unresolved question is whether APC^{Ama1} regulates Ssp1 turnover directly. Although the simplest model would be that APC^{Ama1} ubiquitylates Ssp1 to trigger its degradation, we and others have been unable to identify ubiquitylated forms of Ssp1 in wild type cells (Diamond, unpublished; Maier *et al*., 2007). Furthermore, though the Ssp1 sequence contains matches to both the consensus KEN and D boxes found in many APC substrates, both these sites lie outside the C-terminal domain that has been shown to be required for Ssp1 degradation (Maier *et al*., 2007); and mutation of the KEN box does not produce an obvious phenotype (Diamond, unpublished). Therefore, although the simple model is appealing, it is possible that, analogous to the way in which APC^{Cdc20} regulates cohesin stability through the action of separase (Ciosk *et al*., 1998; Uhlmann *et al*., 1999), APC^{Ama1} acts through some additional protein to regulate Ssp1 turnover.

Another issue still to be addressed is the connection between the failure of cytokinesis in *ama1*Δ and the spore wall phenotype of the mutant. Our FLIP studies reveal that a significant fraction of the prospore membranes in *ama1*Δ cells eventually close, possibly due to slower, *AMA1*-independent turnover of Ssp1. Nonetheless, these prospores do not develop spore walls. In wild-type cells, the onset of spore wall development only occurs after cytokinesis. It may be that the normal closure process generates a signal that initiates wall assembly and this signal is not generated by the abnormal closure of membranes in the *ama1*Δ cells. Alternatively, APC^{Ama1} may have additional roles in spore wall development after cytokinesis. The APC subunit Swm1 was originally identified as a mutant with a spore wall defect (Ufano *et al*., 1999), and an APC subunit has also been identified as a spore wall mutant in *Schizosaccharomyces pombe* (Kakihara *et al*., 2003), suggesting that the APC is important for proper wall assembly. Moreover, *AMA1* has been found to be required for the activation of the mitogen-activated protein kinase Smk1, which regulates spore wall assembly (Krisak *et al*., 1994; Huang *et al*., 2005; McDonald *et al*., 2005). This last observation strongly suggests the existence of additional APC^{Ama1} targets besides Ssp1, and may explain why inactivation of degSsp1 only provides a partial suppression of the *ama1*Δ sporulation defect.

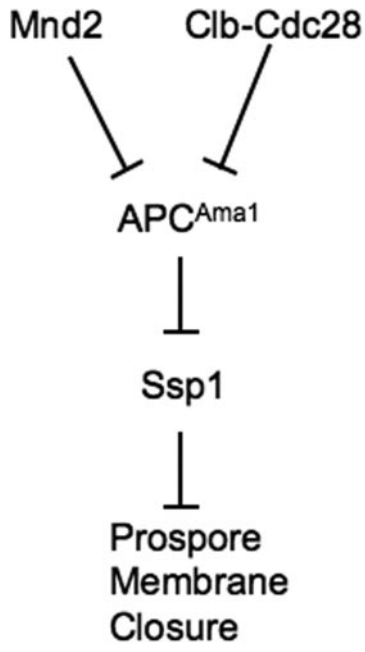

Figure 7. Model for regulatory steps linking completion of meiosis to prospore membrane closure. Mnd2 and Clb-Cdc28 act during early stages of meiosis to restrain APC^{Ama1}. Ssp1 acts as an inhibitor of membrane closure. When Mnd2 and Clb-Cdc28 activities are lost at the end of meiosis II, APC^{Ama1} becomes active and leads to degradation of Ssp1, allowing prospore membrane closure.

Finally, the mechanism by which prospore membrane closure is achieved also requires further exploration. In vegetative yeast cells, cytokinesis is driven by a combination actomyosin ring mediated ingression of the plasma membrane as well as deposition of septal wall material. Neither of these mechanisms is likely to operate in prospore membrane closure as actin is not found at the leading edge, and there is no significant deposition of wall material until well after prospore membrane closure (Coluccio *et al*., 2004; Taxis *et al*., 2006). However, the final separation into distinct cells in a mitotic division requires rearrangement of membrane bilayers and topologically, it represents the same situation as closure of the prospore membrane. Several different membrane fusion associated functions including the exocyst, soluble *N*-ethylmaleimide-sensitive factor attachment protein receptors, and the ESCRT complex have been implicated in this final stage of cell separation during division in multi-

cellular eukaryotes (Lauber *et al*., 1997; Jantsch-Plunger and Glotzer, 1999; Gromley *et al*., 2005; Carlton and Martin-Serrano, 2007). Exactly how division is achieved remains obscure.

Similarly, the mechanism of prospore membrane closure remains to be determined. Ssp1 seems to be antagonistic to membrane fusion (Maier *et al*., 2007), and our data are consistent with the proposal that removal of Ssp1 promotes closure of the membrane, but this leaves open the question of how closure is achieved. Given the parallels to the final stages of cytokinesis in mitotic cells, the identification of proteins that directly mediate closure of the membrane could provide insight into the general mechanism of cytokinesis.

ACKNOWLEDGMENTS

We thank Angelika Amon and Wolfgang Zacharaie (Max Planck Institute, Dresden, Germany) for plasmids, Eva Pablo-Hernando and Bruce Futcher for comments on the manuscript, and Paul Hartley for advice with the degron system. This work was supported by National Institutes of Health grant GM-072540 (to A.M.N.).

REFERENCES

Benjamin, K. R., Zhang, C., Shokat, K. M., and Herskowitz, I. (2003). Control of landmark events in meiosis by the CDK Cdc28 and the meiosis-specific kinase Ime2. Genes Dev. *17*, 1524–1539.

Carlile, T. M., and Amon, A. (2008). Meiosis I is established through division-specific translational control of a cyclin. Cell *133*, 280–291.

Carlton, J. G., and Martin-Serrano, J. (2007). Parallels between cytokinesis and retroviral budding: a role for the ESCRT machinery. Science *316*, 1908–1912.

Christianson, T. W., Sikorski, R. S., Dante, M., Shero, J. H., and Hieter, P. (1992). Multifunctional yeast high-copy-number shuttle vectors. Gene *110*, 119–122.

Chu, S., DeRisi, J., Eisen, M., Mulholland, J., Botstein, D., Brown, P. O., and Herskowitz, I. (1998). The transcriptional program of sporulation in budding yeast. Science *282*, 699–705.

Ciosk, R., Zachariae, W., Michaelis, C., Shevchenko, A., Mann, M., and Nasmyth, K. (1998). An ESP1/PDS1 complex regulates loss of sister chromatid cohesion at the metaphase to anaphase transition in yeast. Cell *93*, 1067–1076.

Coluccio, A., Bogengruber, E., Conrad, M. N., Dresser, M. E., Briza, P., and Neiman, A. M. (2004). Morphogenetic pathway of spore wall assembly in *Saccharomyces cerevisiae*. Eukaryot. Cell *3*, 1464–1475.

Coluccio, A. E., Rodriguez, R., Kernan, M., and Neiman, A. M. (2008). The *Saccharomyces cerevisiae* spore wall allows spores to survive passage through the digestive tract of the fly *Drosophila melanogaster*. PLOS One *3*, e2873.

Cooper, K. F., Mallory, M. J., Egeland, D. B., Jarnik, M., and Strich, R. (2000). Ama1p is a meiosis-specific regulator of the anaphase promoting complex/cyclosome in yeast. Proc. Natl. Acad. Sci. USA *97*, 14548–14553.

Dahmann, C., and Futcher, B. (1995). Specialization of B-type cyclins for mitosis or meiosis in *S. cerevisiae*. Genetics *140*, 957–963.

Dumitrescu, T. P., and Saunders, W. S. (2002). The FEAR Before MEN: networks of mitotic exit. Cell Cycle *1*, 304–307.

Esposito, M. S., Esposito, R. E., Arnaud, M., and Halvorson, H. O. (1970). Conditional mutants of meiosis in yeast. J. Bacteriol. *104*, 202–210.

Esposito, R. E., and Klapholz, S. (1981). Meiosis and ascospore development. In: The Molecular Biology of the Yeast *Saccharomyces*: Life Cycle and Inheritance, ed. J. N. Strathern, E. W. Jones, and J. R. Broach, Cold Spring Harbor, NY: Cold Spring Harbor Laboratory Press, 211–287.

Gao, X. D., Tachikawa, H., Sato, T., Jigami, Y., and Dean, N. (2005). Alg14 recruits Alg13 to the cytoplasmic face of the endoplasmic reticulum to form a novel bipartite UDP-N-acetylglucosamine transferase required for the second step of N-linked glycosylation. J. Biol. Chem. *280*, 36254–36262.

Gromley, A., Yeaman, C., Rosa, J., Redick, S., Chen, C. T., Mirabelle, S., Guha, M., Sillibourne, J., and Doxsey, S. J. (2005). Centriolin anchoring of exocyst and SNARE complexes at the midbody is required for secretory-vesicle-mediated abscission. Cell *123*, 75–87.

Huang, L. S., Doherty, H. K., and Herskowitz, I. (2005). The Smk1p MAP kinase negatively regulates Gsc2p, a 1,3-beta-glucan synthase, during spore wall morphogenesis in. *Saccharomyces cerevisiae*. Proc. Natl. Acad. Sci. USA *102*, 12431–12436.

Huh, W. K., Falvo, J. V., Gerke, L. C., Carroll, A. S., Howson, R. W., Weissman, J. S., and O'Shea, E. K. (2003). Global analysis of protein localization in budding yeast. Nature *425*, 686–691.

Jantsch-Plunger, V., and Glotzer, M. (1999). Depletion of syntaxins in the early *Caenorhabditis elegans* embryo reveals a role for membrane fusion events in cytokinesis. Curr. Biol. *9*, 738–745.

Kakihara, Y., Nabeshima, K., Hirata, A., and Nojima, H. (2003). Overlapping omt1+ and omt2+ genes are required for spore wall maturation in *Schizosaccharomyces pombe*. Genes Cells *8*, 547–558.

Kamieniecki, R. J., Liu, L., and Dawson, D. S. (2005). FEAR but not MEN genes are required for exit from meiosis I. Cell Cycle *4*, 1093–1098.

Kanemaki, M., Sanchez-Diaz, A., Gambus, A., and Labib, K. (2003). Functional proteomic identification of DNA replication proteins by induced proteolysis in vivo. Nature *423*, 720–724.

Katis, V. L., Matos, J., Mori, S., Shirahige, K., Zachariae, W., and Nasmyth, K. (2004). Spo13 facilitates monopolin recruitment to kinetochores and regulates maintenance of centromeric cohesion during yeast meiosis. Curr. Biol. *14*, 2183–2196.

Knop, M., and Strasser, K. (2000). Role of the spindle pole body of yeast in mediating assembly of the prospore membrane during meiosis. EMBO J. *19*, 3657–3667.

Kraft, C., Vodermaier, H. C., Maurer-Stroh, S., Eisenhaber, F., and Peters, J. M. (2005). The WD40 propeller domain of Cdh1 functions as a destruction box receptor for APC/C substrates. Mol. Cell *18*, 543–553.

Krisak, L., Strich, R., Winters, R. S., Hall, J. P., Mallory, M. J., Kreitzer, D., Tuan, R. S., and Winter, E. (1994). SMK1, a developmentally regulated MAP kinase, is required for spore wall assembly in *Saccharomyces cerevisiae*. Genes Dev. *8*, 2151–2161.

Lauber, M. H., Waizenegger, I., Steinmann, T., Schwarz, H., Mayer, U., Hwang, I., Lukowitz, W., and Jurgens, G. (1997). The *Arabidopsis* KNOLLE protein is a cytokinesis-specific syntaxin. J. Cell Biol. *139*, 1485–1493.

Longtine, M. S., McKenzie, A., 3rd, Demarini, D. J., Shah, N. G., Wach, A., Brachat, A., Philippsen, P., and Pringle, J. R. (1998). Additional modules for versatile and economical PCR-based gene deletion and modification in *Saccharomyces cerevisiae*. Yeast *14*, 953–961.

Lynn, R. R., and Magee, P. T. (1970). Development of the spore wall during ascospore formation in *Saccharomyces cerevisiae*. J. Cell Biol. *44*, 688–692.

Maier, P., Rathfelder, N., Finkbeiner, M. G., Taxis, C., Mazza, M., Le Panse, S., Haguenauer-Tsapis, R., and Knop, M. (2007). Cytokinesis in yeast meiosis depends on the regulated removal of Ssp1p from the prospore membrane. EMBO J. *26*, 1843–1852.

Marston, A. L., Lee, B. H., and Amon, A. (2003). The Cdc14 phosphatase and the FEAR network control meiotic spindle disassembly and chromosome segregation. Dev. Cell *4*, 711–726.

Martinez, J. S., Jeong, D. E., Choi, E., Billings, B. M., and Hall, M. C. (2006). Acm1 is a negative regulator of the *CDH1*-dependent anaphase-promoting complex/cyclosome in budding yeast. Mol. Cell. Biol. *26*, 9162–9176.

McDonald, C. M., Cooper, K. F., and Winter, E. (2005). The Ama1-directed anaphase-promoting complex regulates the Smk1 mitogen-activated protein kinase during meiosis in yeast. Genetics *171*, 901–911.

Moens, P. B. (1971). Fine structure of ascospore development in the yeast. *Saccharomyces cerevisiae*. Can. J. Microbiol. *17*, 507–510.

Moens, P. B., and Rapport, E. (1971). Spindles, spindle plaques, and meiosis in the yeast *Saccharomyces cerevisiae* (Hansen). J. Cell Biol. *50*, 344–361.

Moreno-Borchart, A. C., Strasser, K., Finkbeiner, M. G., Shevchenko, A., Shevchenko, A., and Knop, M. (2001). Prospore membrane formation linked to the leading edge protein (LEP) coat assembly. EMBO J. *20*, 6946–6957.

Morgan, D. O. (1999). Regulation of the APC and the exit from mitosis. Nat. Cell Biol. *1*, E47–E53.

Mumberg, D., Muller, R., and Funk, M. (1995). Yeast vectors for the controlled expression of heterologous proteins in different genetic backgrounds. Gene *156*, 119–122.

Nag, D. K., Koonce, M. P., and Axelrod, J. (1997). SSP1, a gene necessary for proper completion of meiotic divisions and spore formation in *Saccharomyces cerevisiae*. Mol. Cell. Biol. *17*, 7029–7039.

Nakanishi, H., de los Santos, P., and Neiman, A. M. (2004). Positive and negative regulation of a SNARE protein by control of intracellular localization. Mol. Biol. Cell *15*, 1802–1815.

Neiman, A. M. (1998). Prospore membrane formation defines a developmentally regulated branch of the secretory pathway in yeast. J. Cell Biol. *140*, 29–37.

Neiman, A. M. (2005). Ascospore formation in the yeast *Saccharomyces cerevisiae*. Microbiol. Mol. Biol. Rev. *69*, 565–584.

Neiman, A. M., Katz, L., and Brennwald, P. J. (2000). Identification of domains required for developmentally regulated SNARE function in *Saccharomyces cerevisiae*. Genetics *155*, 1643–1655.

Nickas, M. E., and Neiman, A. M. (2002). Ady3p links spindle pole body function to spore wall synthesis in *Saccharomyces cerevisiae*. Genetics *160*, 1439–1450.

Oelschlaegel, T., Schwickart, M., Matos, J., Bogdanova, A., Camasses, A., Havlis, J., Shevchenko, A., and Zachariae, W. (2005). The yeast APC/C subunit Mnd2 prevents premature sister chromatid separation triggered by the meiosis-specific APC/C-Ama1. Cell *120*, 773–788.

Ostapenko, D., Burton, J. L., Wang, R., and Solomon, M. J. (2008). Pseudosubstrate inhibition of APCCdh1 by Acm 1, regulation by proteolysis and Cdc28 phosphorylation. Mol. Cell. Biol. *28*, 4653–4664.

Pablo-Hernando, M. E., Arnaiz-Pita, Y., Nakanishi, H., Dawson, D., del Rey, F., Neiman, A. M., and Vazquez de Aldana, C. R. (2007). Cdc15 is required for spore morphogenesis independently of Cdc14 in *Saccharomyces cerevisiae*. Genetics *177*, 281–293.

Penkner, A. M., Prinz, S., Ferscha, S., and Klein, F. (2005). Mnd2, an essential antagonist of the anaphase-promoting complex during meiotic prophase. Cell *120*, 789–801.

Picard, D. (1999). Regulation of heterologous proteins by fusion to a hormone binding domain. In: Nuclear Receptors: A Practical Approach, ed. D. Picard, Oxford, United Kingdom: Oxford University Press, 261–274.

Rabitsch, K. P. *et al*. (2001). A screen for genes required for meiosis and spore formation based on whole-genome expression. Curr. Biol. *11*, 1001–1009.

Rose, M. D., and Fink, G. R. (1990). Methods in Yeast Genetics, Cold Spring Harbor, NY: Cold Spring Harbor Laboratory Press.

Sanchez-Diaz, A., Kanemaki, M., Marchesi, V., and Labib, K. (2004). Rapid depletion of budding yeast proteins by fusion to a heat-inducible degron. Sci. STKE *2004*, PL8.

Schwab, M., Neutzner, M., Mocker, D., and Seufert, W. (2001). Yeast Hct1 recognizes the mitotic cyclin Clb2 and other substrates of the ubiquitin ligase APC. EMBO J. *20*, 5165–5175.

Suda, Y., Nakanishi, H., Mathieson, E. M., and Neiman, A. M. (2007). Alternative modes of organellar segregation during sporulation in *Saccharomyces cerevisiae*. Eukaryot. Cell *6*, 2009–2017.

Tachikawa, H., Bloecher, A., Tatchell, K., and Neiman, A. M. (2001). A Gip1p-Glc7p phosphatase complex regulates septin organization and spore wall formation. J. Cell Biol. *155*, 797–808.

Taxis, C., Maeder, C., Reber, S., Rathfelder, N., Miura, K., Greger, K., Stelzer, E. H., and Knop, M. (2006). Dynamic organization of the actin cytoskeleton during meiosis and spore formation in budding yeast. Traffic *7*, 1628–1642.

Taylor, G. S., Liu, Y., Baskerville, C., and Charbonneau, H. (1997). The activity of Cdc14p, an oligomeric dual specificity protein phosphatase from *Saccharomyces cerevisiae*, is required for cell cycle progression. J. Biol. Chem. *272*, 24054–24063.

Thornton, B. R., Ng, T. M., Matyskiela, M. E., Carroll, C. W., Morgan, D. O., and Toczyski, D. P. (2006). An architectural map of the anaphase-promoting complex. Genes Dev. *20*, 449–460.

Thornton, B. R., and Toczyski, D. P. (2003). Securin and B-cyclin/CDK are the only essential targets of the APC. Nat. Cell Biol. *5*, 1090–1094.

Ufano, S., San-Segundo, P., del Rey, F., and Vazquez de Aldana, C. R. (1999). *SWM1*, a developmentally regulated gene, is required for spore wall assembly in *Saccharomyces cerevisiae*. Mol. Cell. Biol. *19*, 2118–2129.

Uhlmann, F., Lottspeich, F., and Nasmyth, K. (1999). Sister-chromatid separation at anaphase onset is promoted by cleavage of the cohesin subunit Scc1. Nature *400*, 37–42.

Visintin, R., Prinz, S., and Amon, A. (1997). *CDC20* and *CDH1*: a family of substrate-specific activators of APC-dependent proteolysis. Science *278*, 460–463.

Vodermaier, H. C., Gieffers, C., Maurer-Stroh, S., Eisenhaber, F., and Peters, J. M. (2003). TPR subunits of the anaphase-promoting complex mediate binding to the activator protein CDH1. Curr. Biol. *13*, 1459–1468.

Wood, J. S., and Hartwell, L. H. (1982). A dependent pathway of gene functions leading to chromosome segregation in *Saccharomyces cerevisiae*. J. Cell Biol. *94*, 718–726.

Zachariae, W., Schwab, M., Nasmyth, K., and Seufert, W. (1998). Control of cyclin ubiquitination by CDK-regulated binding of Hct1 to the anaphase promoting complex. Science *282*, 1721–1724.